Paper
Int'l J. of Aeronautical & Space Sci. 18(4), 651–661 (2017)
DOI: http://dx.doi.org/10.5139/IJASS.2017.18.4.651

IJASS
International Journal of Aeronautical and Space Sciences

Propulsion System Modeling and Reduction for Conceptual Truss-Braced Wing Aircraft Design

Kyunghoon Lee*
Pusan National University, Busan 46241, Republic of Korea

Taewoo Nam**
Toyota Research Institute of North America, Ann Arbor, MI 48105, USA

Shinseong Kang***
Pusan National University, Busan 46241, Republic of Korea

Abstract

A truss-braced wing (TBW) aircraft has recently received increasing attention due to higher aerodynamic efficiency compared to conventional cantilever wing aircraft. For conceptual TBW aircraft design, we developed a propulsion-and-airframe integrated design environment by replacing a semi-empirical turbofan engine model with a thermodynamic cycle-based one built upon the numerical propulsion system simulation (NPSS). The constructed NPSS model benefitted TBW aircraft design study, as it could handle engine installation effects influencing engine fuel efficiency. The NPSS model also contributed to broadening TBW aircraft design space, for it provided turbofan engine design variables involving a technology factor reflecting progress in propulsion technology. To effectively consolidate the NPSS propulsion model with the TBW airframe model, we devised a rapid, approximate substitute of the NPSS model by reduced-order modeling (ROM) to resolve difficulties in model integration. In addition, we formed an artificial neural network (ANN) that associates engine component attributes evaluated by object-oriented weight analysis of turbine engine (WATE++) with engine design variables to determine engine weight and size, both of which bring together the propulsion and airframe system models. Through propulsion-and-airframe design space exploration, we optimized TBW aircraft design for fuel saving and revealed that a simple engine model neglecting engine installation effects may overestimate TBW aircraft performance.

Key words: Numerical propulsion system simulation, Reduced-order modeling, Artificial neural networks, Propulsion-and-airframe integrated design, Truss-braced wing aircraft

1. Introduction

The truss-braced wing (TBW) configuration, depicted in Fig. 1, was originally conceived by Pfeninger [1] in the 1950s and resurfaced recently as one of the promising next generation aircraft concepts. The high aspect ratio of the TBW is credited to a long and thin, short-chord wing supported by struts and juries for a low weight penalty. This unique wing configuration is conducive to aerodynamic performance enhancement, leading to low environmental footprints incurred by the aircraft. The TBW concept has been investigated by research collaboration between Boeing and NASA under the Subsonic Ultra Green Aircraft Research (SUGAR) program [2]. To examine the feasibility of this innovative configuration, Ref. [3] carried out TBW aircraft design studies mainly focusing on the airframe itself without taking into account propulsion aspects; please refer to Ref. [3] for the details of TBW airframe system modeling.

* Assistant professor and corresponding author: aeronova@pusan.ac.kr
** Research scientist
*** Graduate student

Received: March 28, 2017 Revised: October 25, 2017 Accepted: December 00, 2017

http://ijass.org pISSN: 2093-274x eISSN: 2093-2480

For propulsion system modeling, the previous research in Ref. [3] relied on a semi-empirical turbofan engine model from Ref. [4] dependent on temperature and Mach number assuming current propulsion technology. This simple engine model was expedient; however, it entailed a few drawbacks for TBW aircraft design study.

First, the semi-empirical engine model emulated uninstalled engine performance, and thus it was prone to be inaccurate at high altitudes, particularly those over 36,000 ft., where adverse engine installation effects are evident. For instance, Ref. [6] showed that if installation effects are considered, thrust specific fuel consumption (TSFC) increases, i.e. worsens, as an altitude escalates beyond 36,000 ft.; otherwise, TSFC barely rises with altitude increments. This erroneous engine fuel efficiency predicted by the semi-empirical turbofan engine model is attributed to relatively constant temperature in the lower stratosphere regime. Consequently, Ref. [3] found that the optimal TBW aircraft preferred to cruise at altitudes between 42,000 ft. and 48,000 ft., much higher than the usual cruise altitude of current aircraft, for maximum aerodynamic efficiency. This peculiar TBW aircraft design result would be averted if a physics-based engine model were adopted. Second, the semi-empirical engine model was not complex enough to afford engine cycle parameters to represent a propulsion system architecture; thus, it was inadequate for airframe-and-propulsion integrated design. For that reason, Ref. [3] could not benefit from propulsion design space in exploring the full capability of TBW aircraft. Moreover, the semi-empirical engine model was not amenable to simulating progress in propulsion technology, which resulted in TBW aircraft designed for future deployment, but hinged on turbofan engine technology lagging behind.

To overcome the three issues pertinent to the use of the simple engine model, we developed a thermodynamic cycle-based engine model and assembled it in the TBW design environment implemented with ModelCenter in Ref. [3] based on preliminary investigation conducted in Ref. [7]. For turbofan engine modeling, we utilized the numerical propulsion system simulation (NPSS) [8], propulsion system design and analysis software, to relate engine cycle and thrust parameters to turbofan engine performance data stacked in an engine deck table. In detail, the NPSS inputs comprised six engine parameters, such as fan pressure ratio and combustor exit temperature, and the NPSS output involved four engine responses, such as gross thrust and fuel flow. In addition to the six engine parameters, we included a technology level indicator to account for the effect of advanced propulsion technology on the efficiency of turbofan engine components.

Fig. 1. Notional TBW aircraft configuration created by OpenVSP [5]

Along with the NPSS, we applied object-oriented implementation of weight analysis of turbine engines (WATE) [9], termed as WATE++ [10], to estimate engine size and weight for propulsion and airframe system model integration. The engine parameters of the NPSS model affect 16 engine component attributes, such as high-pressure compressor power and weight, which dictate the drag and weight of a turbofan engine in the airframe system model. To facilitate the incorporation of the NPSS model into the TBW design environment, we capitalized on reduced-order modeling (ROM) to achieve a rapid, approximate NPSS model according to the ROM procedure proposed in Ref. [11]; please see Ref. [11] for the propulsion system modeling and reduction in the context of conceptual aircraft design study. We also formed a functional relationship associating the 16 engine component attributes with the seven turbofan design variables by an artificial neural network (ANN).

In summary, we attempted to examine the TBW aircraft concept through concurrent propulsion and airframe design optimization with the help of a thermodynamic cycle-based turbofan engine model implemented by the NPSS and expedited by ROM. After the introduction, we delineate NPSS turbofan engine modeling as well as NPSS ROM, followed by ANN model construction for engine weight and size estimation. Next, we present results of TBW aircraft design optimization obtained with a propulsion-and-airframe integrated design environment and discuss the consequences of incorrect TSFC prediction by a semi-empirical engine model on TBW aircraft performance. Lastly, we summarize this paper and draw a conclusion on TBW aircraft design study.

2. Propulsion System Modeling

2.1 Turbofan Engine Architecture and Parametrization

For the design of a propulsion system architecture with the NPSS, we chose a two-shaft, separate flow, high bypass turbofan based on the GE90-94B representation implemented for the environmental design space program

[12]. The NPSS turbofan engine model was simulated as a thermodynamic cycle-based model similarly to Ref. [11]. Instead of adopting a rather revolutionary engine, such as hybrid-electric, we employed a state-of-the-art turbofan engine and assumed evolutionary progress of engine component efficiency in the future. To express the efficiency improvement over time, we contrived a technology factor (TF) on a scale of 1 to 10 according to Refs. [4,10] as shown in Table 1. For instance, a TF of 1 denotes the current technology level, and a TF of 10 indicates the anticipated technology level in 2025 in the N+2 timeframe; thus, any TF in-between 1 and 10 implies an anticipated engine component efficiency improvement with respect to the current technology level. We suppose that the use of TF with the NPSS is reasonable because (i) the NPSS engine architecture is a conventional high bypass turbofan, thus historical data is available; and (ii) based on the historical trends in Refs. [4,10], a TF denotes the evolutionary progress of engine component efficiency.

After constructing a turbofan engine model with the NPSS, we set out to determine turbofan engine design variables in consideration of concurrent propulsion and airframe design. As shown in Table 2, we selected a total of seven turbofan engine design variables. The first five variables in Table 2 are engine cycle parameters normally required in the conceptual design phase because they considerably affect

Table 1. Efficiency of turbofan engine components projected as a function of a technology factor [12]

Engine component	Engine component efficiency
Fan	f(FPR[1]) + 0.01 * TF / 10
LPC[2]	f(LPCPR[3]) + 0.03 * TF / 10
HPC[4]	f(HPCPR[5]) + 0.02 * TF / 10
HPT[6]	0.925 + 0.025 * TF / 10
LPT[7]	0.937+ 0.025 * TF / 10

[1] fan pressure ratio
[2] low-pressure compressor
[3] low-pressure compressor pressure ratio
[4] high-pressure compressor
[5] high-pressure compressor pressure ratio
[6] high-pressure turbine
[7] low-pressure turbine

Table 2. Ranges of turbofan engine design variables

Design variable	Minimum	Maximum	Unit
Extraction Ratio	1	1.2	
FPR	1.5	1.7	
HPCPR	18	25	
LPCPR	1.2	1.6	
MaxT4	3,200	3,600	°R
T_{SLS}[1]	50,000	80,000	lbf
TF	1	10	

[1] sea-level static thrust

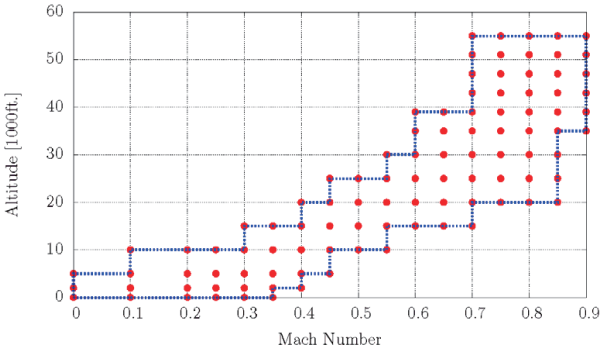

Fig. 2. Turbofan engine operating envelope

engine performance. For example, an extraction ratio and an FPR have a significant influence on an engine bypass ratio (BPR) and thereby sway propulsive efficiency. Both HPCPR and LPCPR have an enormous effect on the overall pressure ratio of an engine, thus dictate thermal efficiency. Similarly, maximum combustor exit temperature, MaxT4, has a large impact on core specific power that determines the overall engine size.

Although the five cycle parameters are germane to engine technology level to some extent, they were treated as engine design variables for TBW aircraft design study. One may argue that the five cycle parameters are the embodiment of technology level. However, a technology level is construed as a factor that extends the limits of the five cycle parameters listed in Table 2. In the context of aircraft design, an engine architecture designer may adjust the cycle parameters such that the resultant engine can fulfill thrust requirements while maximizing engine performance [13]. As such, we controlled the cycle parameters as engine design variables in the TBW aircraft design environment. For an engine operating envelope, we adopted the typical mission profile of a Boeing 777-like civil jet transport, composed of 1089 operating conditions, as depicted in Fig. 2.

2.2 Model Order Reduction of Engine Performance Analysis

Once we constructed a turbofan engine model with the NPSS, we embarked on developing a rapid, approximate substitute of the NPSS model by ROM, as a reduced-order NPSS model is tractable for model integration. The ROM technique, applied to the NPSS model, hinges on a vector space concept such that large dimensional data can be effectively delineated on a small dimensional space by a change of basis. To wit, a reduced-order NPSS model re-expresses engine performance output as a linear combination of a basis weighted by basis coefficients. To evaluate

an orthogonal basis and to estimate basis coefficients, we utilized an expectation-maximization algorithm for probabilistic principal component analysis (EM-PCA) [14] and an ANN, respectively, as demonstrated in Ref. [11]. In the context of our application, a basis represents engine operating conditions, such as a Mach number, an altitude, and a throttle setting, and a basis coefficient accounts for variation in the engine performance data with respect to the seven engine design variables tabulated in Table 2.

For the ROM of the NPSS model, we used a total of 768 and 256 samples to construct and to verify reduced-order NPSS models, respectively, that relate the seven engine design variables to four engine performance data in an engine deck: gross thrust, ram drag, fuel flow, and emission index NOx (EINOx). As with the reduced-order NPSS modeling in Ref. [11], we compiled 768 snapshots of NPSS output to distill them into an empirical orthonormal basis by invoking the EM-PCA. Among 768 basis vectors, we selected two leading basis vectors based on the magnitudes of eigenvalues sorted in descending order, as shown in Table 3, and formed four separate reduced-order NPSS models for each of the four engine performance data; hence, achieving dimensionality reduction from 1089 to 2. Subsequently, we developed basis coefficient prediction models by ANN modeling to associate basis coefficients with the seven engine design variables. For ANN construction, we drew on basic regression analysis for integrated neural networks (BRAINN) [15], ANN modeling software, for it automatically identifies the best ANN architecture by sweeping through the numbers of neurons and layers. As a result, we obtained a single hidden layer feedforward neural network with 40 neurons by BRAINN for basis coefficient estimation.

After reduced-order NPSS modeling, we carried out model verification with the training and testing data in terms of numerical verification metrics, such as a normalized root mean square error (NRMSE), an average of normalized root

Table 3. Cumulative sum of eigenvalues normalized by their sum

Number of eigenvalues	Gross thrust	Ram drag	Fuel flow	EINOx
1	9.8512e-01	9.9624e-01	9.9774e-01	9.9677e-01
2	9.9988e-01	9.9988e-01	9.9966e-01	9.9892e-01
3	9.9992e-01	9.9990e-01	9.9978e-01	9.9953e-01
4	9.9994e-01	9.9993e-01	9.9984e-01	9.9968e-01
5	9.9995e-01	9.9995e-01	9.9989e-01	9.9980e-01

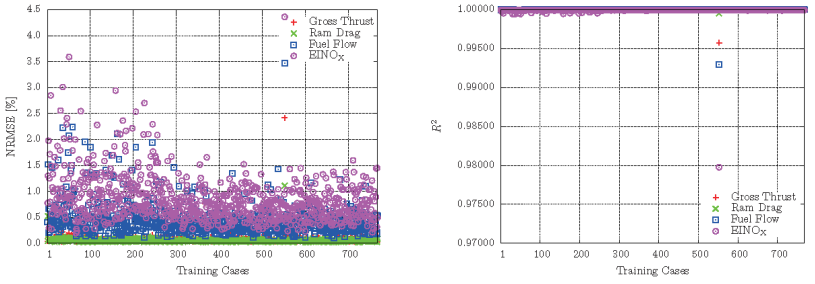

(a) NRMSE (b) R^2

Fig. 3. Numerical verification results of the reduced-order NPSS model with training data

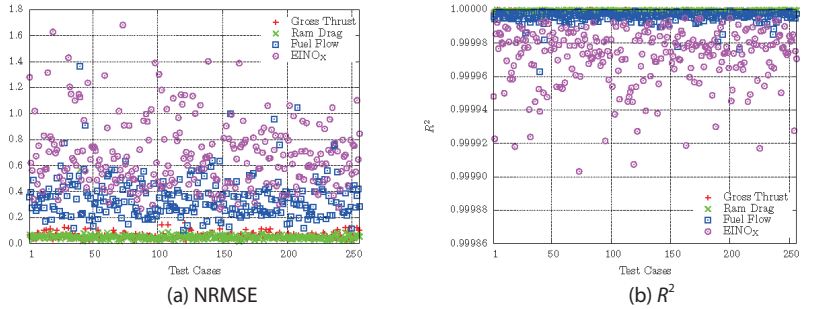

(a) NRMSE (b) R^2

Fig. 4. Numerical verification results of the reduced-order NPSS model with testing data

DOI: http://dx.doi.org/10.5139/IJASS.2017.18.4.651

mean errors (NRSEs), and the coefficient of determination (RSQ). First, we examined the four reduced-order NPSS models against the training data. Fig. 3 shows that most NRMSEs are less than 4% except the 552nd case, which entailed relatively large NRMSEs. Similarly, Fig. 4 exhibits that RSQ values are very close to 1 other than the 552nd case.

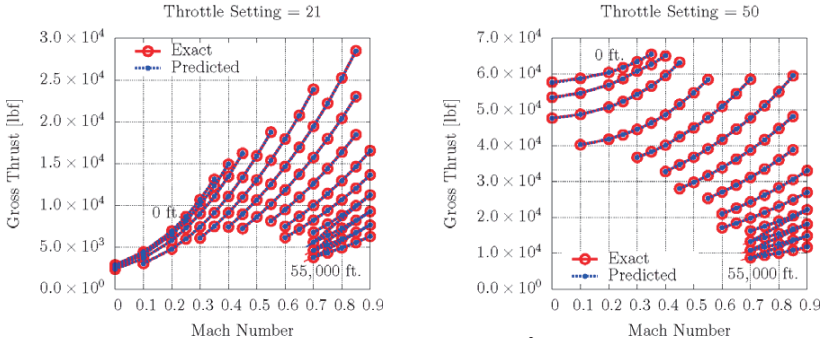

(a) Gross thrust at the 121st testing case: R^2 = 0.9999973

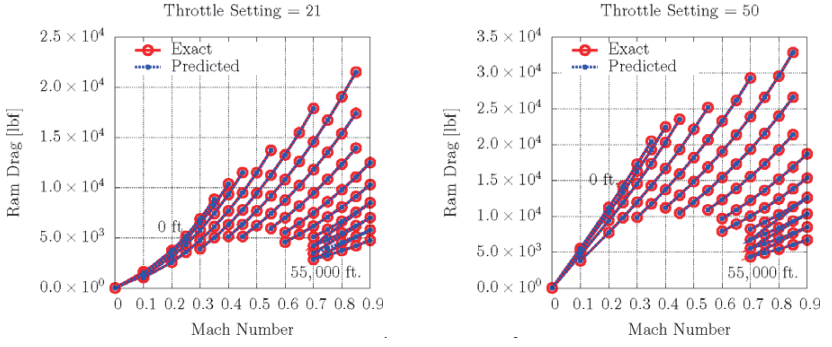

(b) Ram frag at the 40th testing case: R^2 = 0.9999961

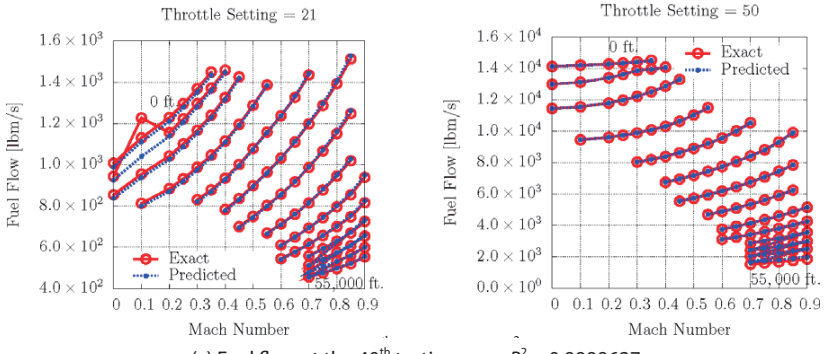

(c) Fuel flow at the 40th testing case: R^2 = 0.9999627

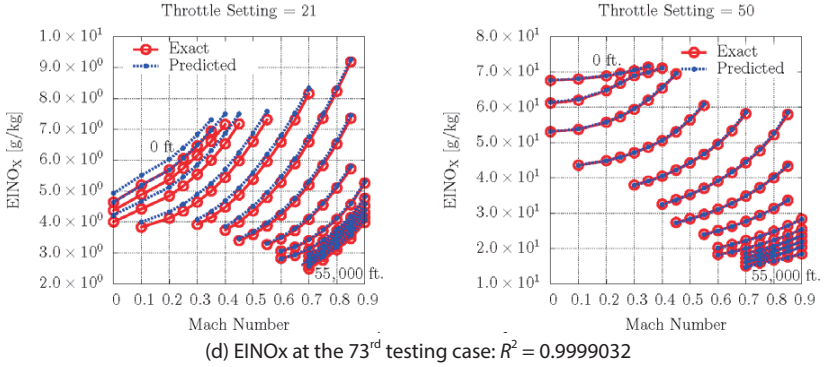

(d) EINOx at the 73rd testing case: R^2 = 0.9999032

Fig. 5. Actual and predicted NPSS performance data of the worst R^2 cases with testing samples

These rather large NRMSE and low RSQ values at the 552nd case were caused by artificial, non-physical simulation errors previously scrutinized in Ref. [11]. Therefore, the abnormal errors do not concern the prediction accuracy of the four reduced-order NPSS models. Next, we repeated the same verification process with the testing data. As shown in Figs. 3 and 4, NRMSE values are less than 1.8%, and RSQ values are greater than 0.9999, respectively. These superb verification results assure that the reduced-order NPSS models predicted engine deck data quite accurately compared to those obtained by the NPSS itself. For further investigation, we inspected the worst RSQ cases as shown in Fig. 5, where the engine performance data predicted by the reduced-order NPSS models agree considerably well with those obtained by the NPSS.

2.3 Weight and Size Estimation of Turbofan Engine Components

In the TBW aircraft design environment, engine size and weight interconnected the propulsion and airframe models. To accordingly estimate the changes of engine size and weight with respect to the engine design variables, we utilized WATE++ [10], then developed ANNs in the form of a single hidden layer feedforward neural network using BRAINN to relate the seven engine design variables to the WATE++ output; namely, 16 engine component attributes as follows: a bypass ratio (BPR); fan power, weight, and corrected weight; high-pressure compressor (HPC) power, weight, and corrected weight; high-pressure turbine (HPT) power, weight, and corrected weight; low-pressure compressor (LPC) power, weight, and corrected weight; and low-pressure turbine (LPT) power, weight, and corrected weight. For training and testing data, we used the same 768 and 256 input samples for the NPSS ROM to generate samples of the 16 engine component attributes. For better function approximation, we meticulously removed the outlier, the 552nd case, in constructing the ANN model with BRAINN. As before, we verified the constructed ANN model with the training and testing samples. As summarized in Table 4, we found that all RSQ values over 0.99 and 0.91 in the cases of training and testing samples, respectively, indicate the reliable prediction capability of the ANN model.

3. Propulsion-Airframe Integrated Truss-Braced Wing Aircraft Design

3.1 Design Optimization Results

In addition to the reduced-order NPSS model, we improved TBW shape rendering with the Geometry Creator and enhanced aircraft performance analysis with the flight optimization system (FLOPS) [16], aircraft sizing and synthesis software. The Geometry Creator substitutes the non-parametric TBW configuration variables in Ref. [3] with parametric ones, such as a wing aspect ratio, and the FLOPS replaces the rudimentary Breguet equation-based performance model in Ref. [3] for more accurate aircraft performance analysis. With the three new analysis components, we revamped the TBW aircraft design environment in Ref. [3] to facilitate propulsion-and-airframe integrated design study.

As an illustration of the overall TBW aircraft design

Table 4. Numerical verification results of the WATE++ ANN model with R2 values

Engine component attribute	Training data	Testing data
BRP	0.999999	0.937483
Fan power	0.999973	0.955606
Fan weight	0.999995	0.990004
Fan corrected weight flow	0.999999	0.990054
LPC power	0.999979	0.993906
LPC weight	0.999999	0.930952
LPC corrected weight flow	0.999912	0.941926
HPC power	0.999979	0.932867
HPC weight	0.999979	0.931448
HPC corrected weight flow	0.999944	0.935787
HPT power	0.999898	0.932132
HPT weight	0.999958	0.927239
HPT corrected weight flow	0.999924	0.963178
LPT power	0.999959	0.958563
LPT weight	0.999974	0.929155
LPT corrected weight flow	0.999913	0.913971

process, Fig. 6 delineates the implemented TBW aircraft design environment in the form of a design structure matrix. In this propulsion-and-airframe integrated design setting, a TBW aircraft is characterized by airframe and engine design variables. The airframe design variables are fed into the Geometry Creator, which defines a TBW configuration. Subsequently, the engine design variables are linked to the reduced-order NPSS model, which sets up a turbofan engine and predicts engine performance metrics. In the propulsion system model, the reduced-order NPSS model is tied up with the WATE++ ANN model, which estimates engine component weights and sizes determining engine weight and drag. Finally, the last FLOPS module predicts the performance metrics of a TBW aircraft, which constitute the objective and constraint functions of a system optimizer for design optimization.

For the TBW aircraft design study, we carried out TBW aircraft design optimization using propulsion and airframe design variables with the mission profile depicted in Fig. 7 for a Boeing 777-like civil jet transport. We addressed TBW aircraft design by nonlinear optimization for minimum block fuel consumption subject to constraints imposed by performance requirements stated in Table 5. To assess the merits of propulsion-and-airframe integrated design space, we first optimized the TBW airframe system with the TBW configuration variables while fixing the propulsion system to

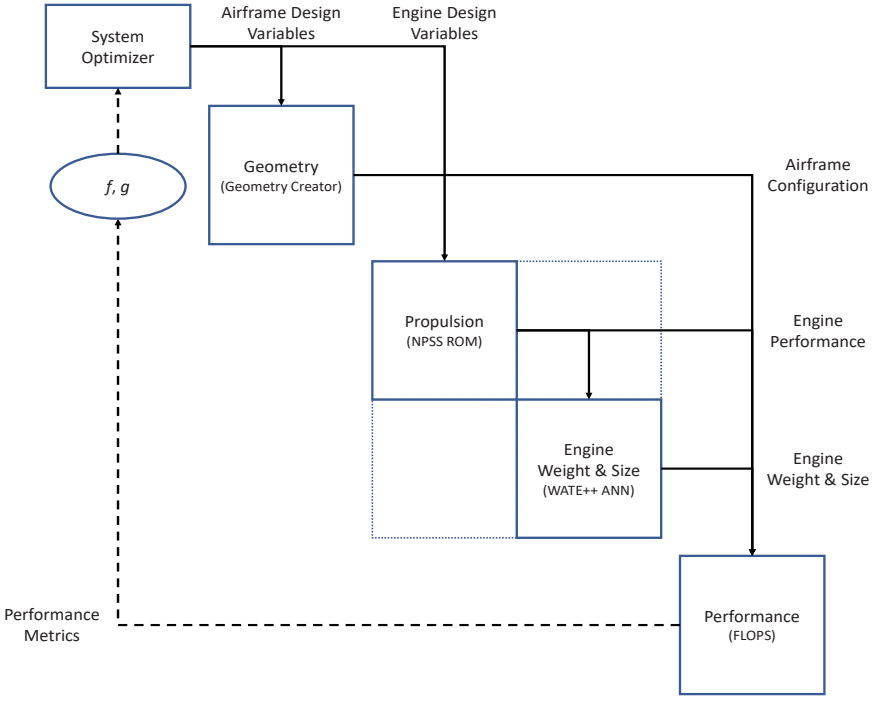

Fig. 6. Overall propulsion-and-airframe integrated design optimization process of a TBW aircraft

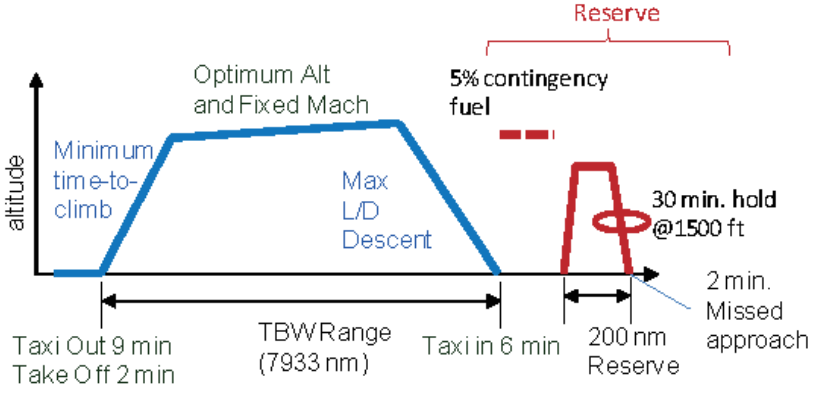

Fig. 7. Mission profile of a TBW aircraft

a GE90-like engine model with a TF of 1. This first optimal TBW aircraft design, termed "Design 1," was obtained only with airframe design space exploration and serves as a baseline for comparative study. Next, we optimized the TBW airframe and turbofan engine systems together with both TBW configuration and engine design variables while holding the TF at 1. This second optimal TBW aircraft design, referred to as "Design 2," was achieved by concurrent airframe and propulsion system design space exploration. Last, we raised the TF of Design 2 to 5 and 10, resulting in "Design 3" and "Design 4," respectively, to evaluate gain from engine technology progress.

After TBW design optimization, we acquired the four optimal TBW configurations depicted in Fig. 8 and summarized the optimal values of the design variables along with their bounds in Table 6. In Table 6, the comparison of Designs 1 and 2 reveals the advantage of enlarged TBW design space through incorporation of propulsion system design space. For instance, the wing area and the sea-level static thrust of Design 1 are smaller than those of Design 2. From Table 6, we can also notice that advanced engine technology, i.e. higher TF values, benefits the TBW airframe design, because Designs 3 and 4 whose TFs are 5 and 10, respectively, have lower wing area and sea-level static thrust than Design 2 whose TF is 1. The smaller wing areas of Designs 2, 3, and 4 attribute to higher wing aspect ratios involved with larger wing aerodynamic efficiency. As for the propulsion system design, Table 6 shows that engine cycle variables are pushed to the limit because of propulsion system design optimization. For example, pressure ratios of high- and low-pressure compressors reached the maximum limit. As a result of engine design optimization, we have obtained turbofan engines with smaller sea-level static thrust, reflecting more efficient turbofan engine architectures, compared to the GE90 representation.

In addition to the design comparison in Table 7, we contrast the relative block fuel reduction of Designs 2, 3, and 4 with respect to Design 1. Table 7 conveys that Design 2 attained a block fuel reduction of 14.75%, which substantiates a distinct advantage accomplished by optimal turbofan engine design. We may further decrease block fuel consumption by 3.66% and 8.00% with Designs 3 and 4 if engine component

Table 5. TBW aircraft design requirements

Performance metrics	Constraint values
Mission range	> 7730 nm
Take-off field length	< 11,000 ft.
Landing field length	< 11,000 ft.
Second segment climb excess thrust (FAR 25, 2.4% climb rate)	> 0 lbf
Missed approach excess thrust	> 0 lbf
Approach speed	< 132.5 knot
Cruise altitude	< 48,000 ft.
Fuel volume margin (available fuel volume – required fuel volume)	> 0 lbf

Table 6. Optimal TBW aircraft design variables and their ranges

Design variables	Design 1	Design 2	Design 3	Design 4	Minimum	Maximum	Unit
Aspect ratio	20.64	23.61	25.00	25.00	10	25	
Wing area	5118	4804	4814	4674	3000	5000	$ft.^2$
Wing weep angle	30.0	30.0	30.0	30.0	15	30	°
Strut/Wing intersection	0.58	0.60	0.59	0.59	0.4	0.75	
Jury/Wing intersection	0.48	0.46	0.46	0.46	0.3	0.8	
Jury/Strut intersection	0.48	0.38	0.39	0.40	0.3	0.8	
Extraction ratio	1.08	1.00	1.00	1.00	1.0	1.2	
FPR	1.58	1.50	1.50	1.50	1.5	1.7	
HPCPR	20.7	22.0	22.0	22.0	18	22	
LPCPR	1.3	1.6	1.6	1.6	1.2	1.6	
MaxT4	3450	3600	3600	3600	3200	3600	°R
T_{SLS}	69002	61646	61681	62191	50000	80000	lbf

technology progresses to TF levels of 5 and 10, respectively. If the anticipated fuel reduction is not sufficient, we need to resort to an alternative propulsion system architecture other than a conventional turbofan engine.

3.2 Engine Installation Effect Investigation

Unlike the semi-empirical turbofan engine model employed in Ref. [3], an NPSS turbofan engine model can properly simulate engine installation effects resulting in engine performance degradation at high altitudes. To delve into the consequence of engine installation effects on TBW aircraft design, we examined TBW aircraft performance in terms of the optimal cruise altitude and the specific air range (SAR) with respect to maximum takeoff weight (MTOW) variation. For this analysis, we used the TBW aircraft designed for minimum fuel burn, i.e. Design 1, as a datum and emulated TSFC of a semi-empirical turbofan engine by leveling TSFC of the NPSS turbofan engine model if the altitude was higher than 36,089 ft. Fig. 9 illustrates the two distinct TSFC trends evaluated with a maximum throttle setting at Mach 0.8.

First, Fig. 10(a) shows that optimal cruise altitudes for maximum SAR achieved in consideration of engine installation effects are consistently lower than those obtained without engine installation effects, which accord closely with our predictions based on real turbofan engine behavior. Because of a decrease in the optimal cruise altitude due to engine installation effects, reduction in aerodynamic efficiency is inevitable at the optimal cruise altitude, as air density is inversely proportional to altitude. Consequently,

Table 7. Block fuel conserved by optimal TBW aircraft designs

TBW aircraft	Block fuel reduction [%]
Design 2	14.75
Design 3	18.42
Design 4	22.76

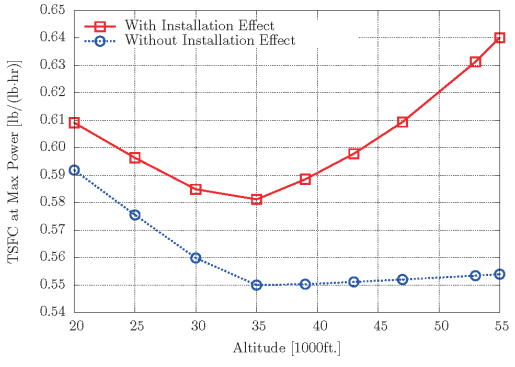

Fig. 9. Engine installation effects on TSFC

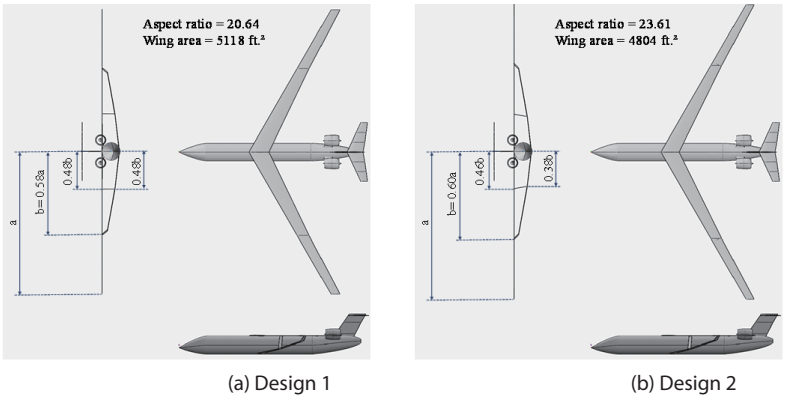

(a) Design 1 (b) Design 2

(c) Design 3 (d) Design 4

Fig. 8. Optimal TBW aircraft design configurations

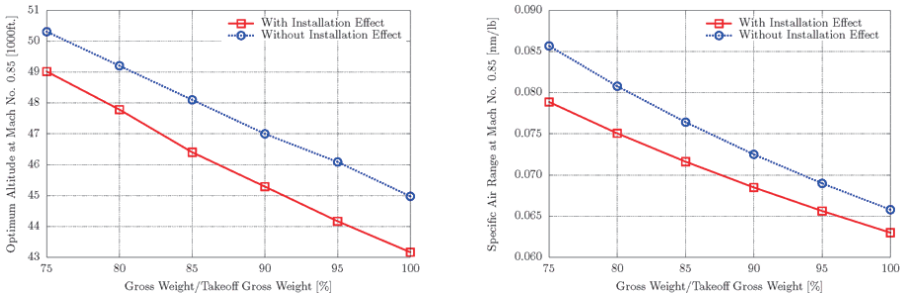

(a) Optimal cruise altitude (b) Specific air range

Fig. 10. Engine installation effects on a TBW aircraft design

Fig. 10(b) shows that engine installation effects cut down an SAR, which implies that a designed aircraft can cover less mileage for the same amount of fuel. Through the comparative study, we found that we may inadvertently aggrandize the performance of designed TBW aircraft if we adopt a semi-empirical turbofan engine model that cannot properly account for engine installation effects.

4. Conclusion

In lieu of a semi-empirical turbofan engine model, we leveraged the thermodynamic cycle-based turbofan engine model using the NPSS to investigate not only airframe but also propulsion design space to grasp the full potential of the TBW aircraft concept. To ease the integration of airframe and propulsion models, we applied reduced-order and ANN modeling to the NPSS and WATE++ models, respectively. Thanks to the propulsion system model augmented to the TBW design environment, TBW aircraft optimized for minimum block fuel consumption achieved lower wing areas and smaller sea-level static thrust compared to the one optimized only with the airframe model. Moreover, the concurrent airframe and propulsion system design approach resulted in TBW aircraft conserving 14.75% more block fuel, which can further increase up to 22.76% through engine technology advancement. Overall, we probed the possible benefits of the TBW design concept with respect to fuel saving with a contemporary turbofan engine presuming evolutionary propulsion technology progress. Future research on TBW aircraft design may utilize unconventional propulsion system architectures, such as hybrid electric-gas turbine engines.

Acknowledgement

This research was supported by the Engineering Research Center Program and the Basic Science Research Program through the National Research Foundation of Korea (NRF) funded by the Ministry of Education, Science, and Technology (No. 2012R1A5A1048294) and the Ministry of Education (No. NRF-2016R1D1A1B03930126), respectively. The authors would like to express sincere gratitude to Drs. Ohad Gur and Manav Bhatia as well as Professor Dimitri Mavris and Mr. Christopher Perullo for their contributions to the TBW aircraft design environment.

References

[1] Pfenninger, W., "Laminar Flow Control Laminarization", AGARD special course on concepts for drag reduction, AGARD Report No. 654, June 1977.

[2] Bradley, M. K. and Droney, C. K., "Subsonic Ultra Green Aircraft Research Phase II: N+ 4 Advanced Concept Development", Tech. Rep. NASA/CR-2012-217556, NASA Langley Research Center, 2012.

[3] Gur, O., Bhatia, M., Schetz, J., Mason, W., Kapania, R. and Mavris, D., "Design Optimization of a Truss-Braced-Wing Transonic Transport Aircraft", *Journal of Aircraft*, Vol. 47, No. 6, November–December 2010, pp. 1907-1917.

[4] Mattingly, J. D., Heiser, W. H. and Pratt, D. T., *Aircraft Engine Design 2nd ed. (AIAA Education)*, AIAA, December 2002.

[5] Hahn, A., "Vehicle Sketch Pad: Parametric Geometry for Conceptual Aircraft Design", *48th AIAA Aerospace Sciences Meeting*, Orlando, FL, Jan 4–7 2010, AIAA-2010-657.

[6] Bullock, R. O., "Analysis of Reynolds Number and Scale Effects on Performance of Turbomachinery", *ASME, Journal of Engineering for Power*, 1964, pp. 247-256.

[7] Lee, K., Perullo, C., Nam, T., Mavris, D. N. and Schetz, J., "Integrated Propulsion and Airframe System Modeling and Analysis for a Truss-Braced Wing Configuration", *20th International Society for Air Breathing Engines (ISABE)*

Conference, Gothenburg, Sweden, September 15, 2011.

[8] Veres, J. P., "Overview of High-Fidelity Modeling Activities in the Numerical Propulsion System Simulations (NPSS) Project", Tech. Rep. NASA/TM-2002-211351, NASA Glenn Research Center, Cleveland, Ohio 44135, June 2002.

[9] Onat, E. and Klees, G. W., "A Method to Estimate Weight and Dimensions of Large and Small Gas Turbine Engines", Tech. Rep. NASA-CR-159481, NASA, January 1, 1979.

[10] Tong, M. T. and Naylor, B. A., "An Object-Oriented Computer Code for Aircraft Engine Weight Estimation", Technical Memorandum NASA/TM-2009-215656, Glenn Research Center, Cleveland, Ohio 44135-3191, December 2009, prepared for the Gas Turbine Technical Congress and Exposition (Turbo Expo 2008) sponsored by the American Society of Mechanical Engineers Berlin, Germany, June 9-13, 2008.

[11] Lee, K., Nam, T., Perullo, C. and Mavris, D. N., "Reduced-Order Modeling of a High-Fidelity Propulsion System Simulation", *AIAA Journal*, Vol. 49, No. 8, August 2011, pp. 1665-1682.

[12] Kirby, M. R. and Mavris, D. N., "The Environmental Design Space", *ICAS 2008-4.7.3*, 2008.

[13] Ballal, D. R. and Zelina, J., "Progress in Aero-Engine Technology (1939–2003)", *In 39th AIAA/ASME/ASEE Joint Propulsion Conference and Exhibit*, No. AIAA-2003-4412, 2003.

[14] Tipping, M. E. and Bishop, C. M., "Probabilistic Principal Component Analysis", *Journal of the Royal Statistical Society: Series B (Statistical Methodology)*, Vol. 61, No. 3, 1999, pp. 611-622.

[15] Johnson, C. and Schutte, J., "Basic Regression Analysis for Integrated Neural Networks (BRAINN) Documentation", Aerospace Systems Design Laboratory (ASDL), January 31, 2009, Version 2.3.

[16] Mccullers, L. A., "Aircraft Configuration Optimization Including Optimized Flight Profiles", NASA Langley Research Center, January 1, 1984.